RESEARCH ARTICLE

AFRICAN ENTOMOLOGY

Revised description of the blueberry bud mite, *Acalitus vaccinii* (Acari: Trombidiformes: Eriophyidae), and a key to all Eriophyoidea on *Vaccinium*

NP Ngubane-Ndhlovu[1,2]* (iD), **I Dhanani[1]**, **F Roets[2]** (iD) **and DL Saccaggi[1,3]** (iD)

[1]*Plant Health Diagnostic Services, Department of Agriculture, Land Reform and Rural Development (DALRRD), Stellenbosch, South Africa.*
[2]*Department of Conservation Ecology and Entomology, Stellenbosch University, Stellenbosch, South Africa.*
[3]*Citrus Research International, Stellenbosch University, Stellenbosch, South Africa.*

In 2014 the blueberry bud mite, *Acalitus vaccinii* (Acari: Trombdiformes: Eriophyidae), was detected causing significant damage to cultivated blueberries in the Mpumalanga province of South Africa. This was the first detection of this pest outside of North America, to which it is native. However, its taxonomic description at that time lacked critical detail and omitted characters and life stages important for easy and accurate identification. Using an integrative taxonomic approach, we combined phase contrast light microscopy with low-temperature SEM and DNA barcoding data to revise the description of A. vaccinii using South African specimens. Additional characters not included in previous descriptions but reported here are the h1 (accessory) setae, leg I and II u' (mesal) setae, and leg II bv (femoral) setae. Detailed descriptions and measurements of all life stages are included, along with a discussion of morphological variation and biology. Two DNA sequences of common barcode regions (nuclear and mitochondrial) are provided to further aid in identification. In addition, a key to all known species of eriophyoid mites present on Vaccinium is provided.

INTRODUCTION

Blueberries, *Vaccinium* spp. (Ericaceae), have become a rapidly expanding commercial crop in South Africa since the 1980s. Most commercial blueberry plantations are in the Western Cape province, where the longer winters contribute to better berry yield (Meyer and Prinsloo 2003). South African blueberry plantations have been relatively free of pests until 2012 when *Acalitus vaccinii* (Keifer 1939) (Trombidiformes: Eriophyidae), the blueberry bud mite, was discovered for the first time in South Africa on a farm in the Mpumalanga province. It was identified as such based on the original and subsequent species descriptions, and by comparison to other eriophyoids known on *Vaccinium* spp., and to other *Acalitus* spp. known from Africa. The mite caused substantial damage that resulted in an estimated 80% decreased yield within only two years of its detection. Symptoms included red blistering on buds, production of small leaves and fruit, as well as malformed flowers (Craemer 2018). Further surveys by the South African Department of Agriculture, Land Reform and Rural Development (DALRRD) also confirmed blueberry bud mite infestations in other locations within the Mpumalanga and North West provinces (Ngubane-Ndhlovu et al. 2018)

Acalitus vaccinii is part of the superfamily Eriophyoidea, casually referred to as eriophyoid mites. Eriophyoidea contains three families, namely Eriophyidae, Diptilomiopidae and Phytophtidae. Eriophyoid mites are highly specialised, plant-feeding and are typically host-specific. These mites are minute, between 100 and 300 μm long with worm-like bodies and two pairs of legs. Many species are of commercial interest as they can cause malformation of buds, can form galls, or cause rust-like symptoms on leaves and fruit.

The lifecycle of *A. vaccinii* is typical for eriophyoid mites and includes eggs, larvae, nymphs, and adult males and females. Two female forms can be present, a deutogyne hibernating winter form and protogyne sexually active summer form. In *A. vaccinii*, the presence of a deutogyne has been noted in the colder areas of its native range in North America (Manson and Oldfield 1996; Cromroy and Kuitert 2001). The identification of both forms is important for assigning species identity to eriophyoid mites, where misidentification of the deutogyne is frequent (Zhao 2000; Smith et al. 2010; Guo et al. 2015). As is the case with many eriophyoids, accurate identification of *A. vaccinii* is hampered by incomplete species descriptions, inaccurate description of some characters and life stages in original descriptions and a lack of identification keys. For example, no comprehensive key to the >90 *Acalitus* species worldwide or to the nine eriophyoids on *Vaccinium* spp. (one Diptilomiopidae and eight Eriophyidae) exist.

Acalitus vaccinii was first described by Keifer (1939) as *Eriophyes vaccinii*, but later moved to *Aceria* (Keifer 1946) and thereafter to *Acalitus* (Baker and Neunzig 1970). In this paper we used modern methods to examine *A. vaccinii* and revise its description, including originally missed characters and all developmental stages. For enhanced clarity, specimens are examined using two imaging techniques, namely phase-contrast light microscopy (PCLM) and low-temperature scanning electron microscopy (LT-SEM) to scrutinise characters on slide-mounted and in situ mites. We also aim to provide diagnostic DNA barcoding sequences including nuclear (28S) and mitochondrial

(COI) regions of *A. vaccinii* to accompany morphological descriptions and to increase accuracy of future identifications of this important pest. Additionally, we provide an identification key to eriophyoid species on *Vaccinium* worldwide.

METHODS

Mite collection

Plant material showing symptoms of *A. vaccinii* infestation was collected from farms near three different towns in the Mpumalanga province in South Africa (Table 1). On each farm at each sampling occasion, 30 samples of 30 cm long shoots were taken at random per cultivar and per block and placed in resealable plastic bags. These shoot samples were kept at 4 °C until examination for the presence of eriophyoids using a stereomicroscope. For traditional microscopic examination using a compound microscope, eriophyoids were collected into a drop of sorbitol and isopropyl-alcohol solution until mounting (de Lillo et al. 2010). For scanning electron microscopy (SEM), mites were kept in situ until preparation. For molecular analysis, eriophyoids were placed into a drop of distilled water on a glass slide and processed immediately.

Morphological examination

Phase contrast light microscopy (PCLM)

Collected eriophyoids were mounted on glass slides using F-medium following published protocols (Keifer 1975; de Lillo et al. 2010). Specimens were examined at 1 000× magnification using a Zeiss Axioskop Imager M2 microscope (Zeiss, Germany), equipped with a drawing tube and Zeiss AxioCam Cc5 digital camera. ZEN 2012 software was used for line drawings and capturing of images. Seventy-five characters for females, 69 for males and 68 for immatures were measured using a Leica DM 2500 microscope (Leica Weitzlar, Germany) connected to a Leica digital camera and Leica application suite v 3.1.0 software.

Principal component analysis (PCA)

To determine if distinctive clusters of characters were present, we performed a principal component analysis using morphological characters of 11 females collected from different seasons (six in summer and five in winter) (Table S1). From the initial 75 morphological characters measured, only independent and non-repeated characters which showed a standard deviation greater than one were used, resulting in 28 characters used in the PCA. PCA was performed in Rstudio v.1.1.447 running R statistical analysis v.3.5.0 (R Core Team 2020; R Studio Team 2020). To visualise the results, the packages *ggfortify* (Tang et al 2016; Horikoshi and Tang 2018) and *ggplot2* (Wickham 2016) were used. Slide-mounted voucher material of all stages were deposited in the mite collection of DALRRD, Plant Quarantine

Station in Stellenbosch, South Africa, and in the National Collection of Arachnida – Acari of the Agricultural Research Council – Plant Health and Protection, in Pretoria, South Africa.

Scanning electron microscopy (SEM)

A modified version of the cryo-fixation technique described by Echlin et al. (1970) was used for preparing specimens and studying them with a conventional JEOL JSM 840 SEM with a cryo-stage. Fourteen females, two males, two nymphs and two larvae were mounted on double-sided carbon tape. The tape was attached in a specimen holder with silver paint, which was plunge-frozen in liquid nitrogen slush and then transferred via the pre-chamber of the cryo-system to the pre-cooled cryo-stage in the chamber of the SEM (*ca.* –170 °C). Here the specimen was etched for *ca.* 30 minutes by increasing the temperature to *ca.* –80 °C to remove ice crystals. The specimen holder was then transferred back to the pre-chamber and sputter-coated with gold, then returned to the cryo-stage for observation of specimens at an accelerating voltage of 5 kV or 2 kV (to prolong viewing time). Digital images were captured using a frame grabber controlled by Orion[*] 6.6.

Revised description of Acalitus vaccinii

Identification was confirmed based on species-specific microscopic characters according to Keifer (1939, 1946) and Baker and Neunzig (1970). A revised description of *A. vaccinii* is presented following the recommendations of Amrine and Manson (1996) and De Lillo et al. (2010). All measurements are given in micrometers (μm), rounded off to the nearest integer, as a range (minimum to maximum). Measurements refer to the length (not width) of the morphological character unless specified otherwise. Terminology follows that of Lindquist (1996).

Identification key

An identification key to all Eriophyoidea species known from *Vaccinium* spp. worldwide was compiled. The key was adapted from published literature (Amrine et al. 2003; Lindquist and Amrine 1996) and original species descriptions (Keifer 1939, 1940, 1953, 1971; Roivainen 1947, 1951; Wei et al. 2009).

Genetic analyses

DNA extraction

Groups of four to eight live mites were crushed in a small drop of distilled water on a glass slide. Using a micropipette, the drop containing the mites was then transferred into a sterile microcentrifuge tube for DNA extraction. DNA extractions were performed using a Qiagen QIAamp DNA Micro Kit (Qiagen, California, USA) following the manufacturer's instructions with the exception that all reaction volumes were halved to improve

Table 1. Location and collection information of blueberry plantations from which *Acalitus vaccinii* was collected from November 2014 to November 2016

Site* and collection times	GPS location of town*	Size of blueberry plantation	Blueberry species	Cultivars	Age of plantation
Dullstroom (Nov 2015; Dec 2016)	25.4184° S, 30.1041° E	4 ha	*Vaccinium corymbosum*	'Elliott'	4 yrs
			Vaccinium corymbosum	'Elliott'	8 yrs
Lydenburg (Nov 2015; Dec 2015; Aug 2016; Dec 2016)	25.0816° S, 30.4473° E	3 ha	*Vaccinium virgatum*	'Climax'	25 yrs
			Vaccinium virgatum	'Delite'	25 yrs
	26.4051° S, 30.4473° E	10 ha	*Vaccinium corymbosum*	'Bluecrop'	6 yrs
			Vaccinium corymbosum	'Berkley'	14 yrs
Amsterdam (Nov 2014; Jul 2015; Nov 2015; Aug 2016; Nov 2016)			*Vaccinium corymbosum*	'Elliott'	14 yrs
			Vaccinium corymbosum	'Spartan'	14 yrs
			Vaccinium virgatum	'Centurion'	14 yrs

*Due to confidentiality of information, sites are named in this study according to the nearest town. GPS coordinates also refer to the nearest town.

DNA concentration. The DNA extractions were eluted into final volumes of 30 μl and stored at –20 °C.

DNA amplification and sequencing

PCR reactions were performed in 25 μl volumes on a Techne Prime Thermal Cycler (Staffordshire, UK). Amplification was performed using 6 μl of DNA extract with half volumes of Promega Corporation (Madison, WI) GoTaq DNA polymerase, following manufacturer's instructions.

A 657 bp segment of the D2 domain of the nuclear 28S rDNA gene was amplified via nested PCR following the protocol of Chetverikov et al. (2019) (Table 2), with an additional 1.5 μl 25 mM MgCl$_2$ per reaction in both PCR reaction mixes to increase the rate of amplification. PCR products were sequenced using the primers from step two. PCRs using the conventional COI barcoding primers (LCO1490 and HCO2198, Folmer et al. 1994) failed to amplify under a range of conditions. Instead, a 417 bp segment of the 5' end of COI was amplified using the available COI primers (Simon et al. 1994; Hedin and Maddison 2001) (Table 2). PCR reactions for COI contained an additional 1.0 μl 25 mM MgCl$_2$ and 1.0 μl 10 mM dNTP mix to boost amplification while minimising mis-priming. Cycling conditions are provided in Table 2. All PCR products were viewed by electrophoresis on a 1.5% agarose gel. DNA sequencing was performed by Inqaba Biotech (Pretoria, South Africa). Trace files were checked, edited, and prepared for submission to GenBank using MEGA v.11.0.13 (www.megasoftware.net). Both sets of sequences were compared to eriophyoid sequences available in GenBank (18 January 2024) using blastn and blastx (for COI) algorithms (http://blast.ncbi.nlm.nih.gov/Blast.cgi).

RESULTS
Revised description
Superfamily: ERIOPHYOIDEA Nalepa, 1898
Family: Eriophyidae Nalepa, 1898
Subfamily: Eriophyinae Nalepa, 1898
Tribe: Aceriini Amrine and Stasny, 1994
Genus: *Acalitus* Keifer, 1965

Acalitus vaccinii (Keifer 1939)

Eriophyes vaccinii Keifer 1939: 328–345, figure: plate LXIX (original designation)
Aceria vaccinii (Keifer) Keifer 1946: 568, (no images)
Keifer 1965:2, figure: plate 1
Acalitus vaccinii (Keifer) Baker and Neunzing 1970: 74–79, figure 4–7.
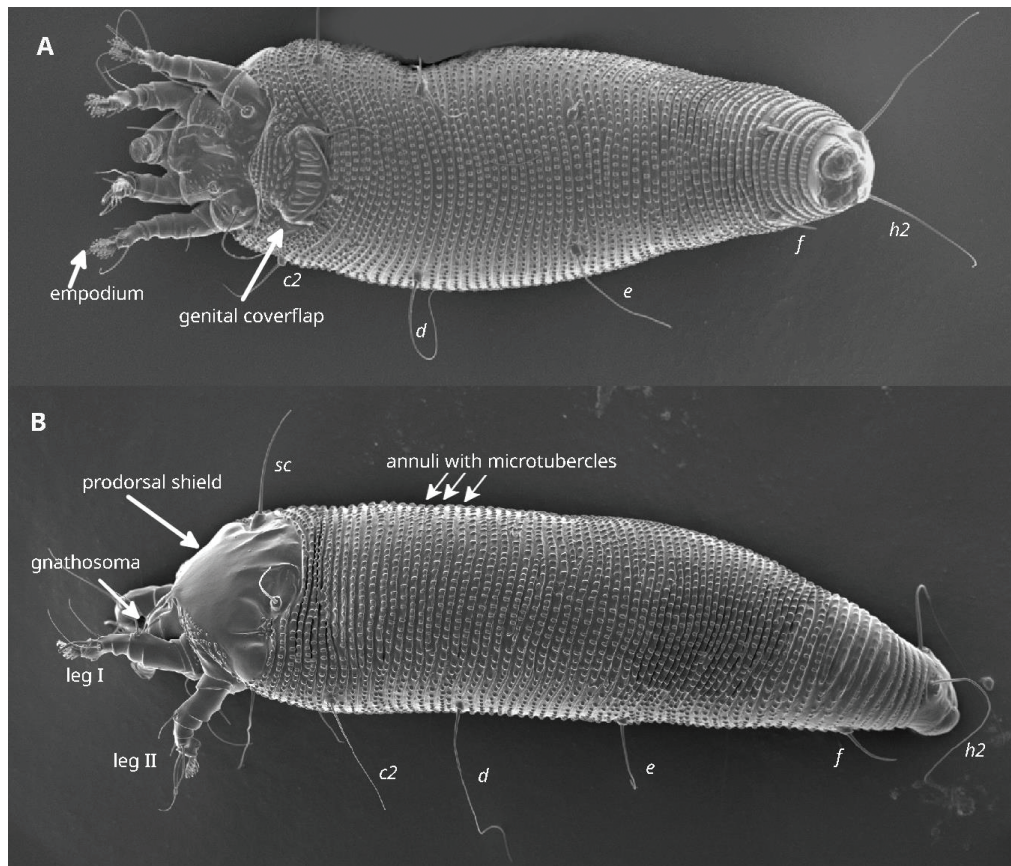
Female

(Figures 1–7) ($n = 11$)

Idiosoma: (Figure 1 and 2) Whitish, wormlike body 167–261 including pedipalp, 150–233 excluding gnathosoma, 48–63 wide (at the level of *c2* setae). Opisthosoma dorsally arched with 65–88 dorsal and 57–72 ventral microtuberculate annuli (from first annulus posterior to coxae II). Dorsally and ventrally with round to oval microtubercles, ventrally gradually elongated towards the rear, dorsally becoming more elongated and vague (probably subsurface) towards the rear until spiny microtubercles protruding from the posterior annulus margins of the telosome. Opisthosomal seta *c2* 21–33 on ventral annulus 10–11, 46–57 apart; opisthosomal seta *d* 30–52 on ventral annulus 21–24, 35–49 apart; opisthosomal seta *e* 33–46 on ventral annulus 35–40, 24–31 apart; opisthosomal seta *f* 11–17, on annulus 5–6 from the rear, 15–18 apart, fine at apex. Opisthosomal setae *h1*, minute, less than 0.5. Opisthosomal setae *h2* 46–59, finely tapered.

Gnathosoma: (Figure 3) 17–23, directed forward and slightly downward, basal part covered by small, pointed frontal lobe, chelicerae 18–25, palp coxal seta *ep* 4–6, apico-ventral setae *v* 2, palp genual setae *d* absent.

Prodorsal shield: (Figure 4) oval, 23–28 long, 31–50 wide; frontal lobe small, thin, anteriorly pointed or slightly rounded. Prodorsal shield with pair of usually obscure admedian lines on posterior ¼ of shield between scapular *sc* setae, more or less curving outwards from rear, then curving inwards, few granules on the outer side of scapular tubercles, with eye-like structures on their outer side partly margined with single rounded, shallow

Table 2. DNA markers, PCR primers and cycling conditions used for amplification and sequencing of *Acalitus vaccinii* specimens in this study. F/R indicates a forward (F) or reverse (R) primer. Accession numbers for sequences submitted to GenBank are included. Extractions are from the Dullstroom (D) and Lydenburg (E) populations.

Locus	Primer	F/R	Primer sequence 5'-3'	Cycling conditions	Reference	GenBank accession	Isolate
28S (step 1)	f1230	F	TGAAACTTAAAGGAATTGACG	95 °C for 3 m	Dabert et al. 2010	MW246114	D2
	D1D2rev4_E	R	GTTAGACTCCTTGGTCCGTG	95 °C for 30 s	Sonnenberg et al. 2007	MW246115	D3
				52 °C for 30 s ⎤ ×30		MW246116	D4
				72 °C for 3 m ⎦			
				72 °C for 9 m			
28S (step 2)	D1D2fw2_E	F	ACAAGTACCGTGAGGGAAAGTTG	95 °C for 1 m	Chetverikov et al. 2019		
	28SR_990	R	CCTTGGTCCGTGTTTCAAGAC	95 °C for 30 s	Mironov et al. 2012		
				62 °C for 30 s ⎤ ×30			
				72 °C for 3 m ⎦			
				72 °C for 9 m			
COI partial barcode	C1-J-2183	F	CAACATTTATTTTGATTTTTTGG	95 °C for 1 m	Simon et al. 1994	MW250771	D2
(region 1)	C1-N-2568	R	GCWACWACRTAATAKGTATCATG	95 °C for 30 s	Hedin and Maddison 2001	MW250772	D3
				50 °C for 45 s ⎤ ×33		MW250773	D4
				72 °C for 1 m ⎦			
				72 °C for 10 m			

Figure 1. SEM image of the opisthosoma (body) of *A. vaccinii* protogyne female, showing the ventral (A) and dorsal (B) aspect. Annuli are the rings around the body, and microtubercles are the protrusions on these rings (more detail can be seen in Figure 2). SEM images were cropped to show the region of interest. For sizes of structures, refer to the measurements included in text.

ridge, band of granules on outer margins of shield and on epicoxal area (sensu Chetverikov and Craemer 2015). Scapular setae *sc* 20–24, 22–25 apart, projecting posteriad.

Leg I: (Figure 5 and 6) all usual segments present, 20–25; trochanter 4–5, femur 3–7, basiventral femoral seta *bv* absent, genu 3, antaxial genual seta *l″* 17–23; tibia 3–5, paraxial tibial seta *l′* absent; tarsus 4–6, paraxial unguinal tarsal seta *u′* 1–3, paraxial fastigial tarsal seta *ft′* 12–18, antaxial fastigial tarsal seta *ft″* 5–9. Tarsal solenidion ω 5–7, slightly curved, sometimes straight and slightly knobbed, tarsal empodium *em* 4–6, simple, symmetrical, 6-rayed.

Leg II: (Figure 5 and 6) all usual segments present, 19–21; trochanter 3–5, femur 3–6, basiventral femoral seta *bv* 4–7, genu 2–4, antaxial genual seta *l″* 19–21; tibia 3–6, tarsus 4–5, paraxial unguinal tarsal seta *u′* 2–3, paraxial fastigial tarsal seta *ft′* 14–20, antaxial fastigial tarsal seta *ft″* 4–9. Tarsal solenidion ω 6–8, slightly curved, sometimes straight, and slightly knobbed. Empodium *em* 4–6, simple, symmetrical, 6-rayed.

Coxisternal area: (Figure 7) suboral plate rounded, with few granules and three slight longitudinal elevations medially (only visible with SEM). Coxisternal plates I and II ornamented with rounded to elongated granules, granules arranged in single row, parallel to and close to margin between coxisternal plates and leg trochanters. Anterolateral setae on coxisternal plate I *1b* 5–7, 7–10 apart, proximal setae on coxisternal plate I *1a* 20–25, 12–16 apart, proximal setae on coxisternal plate II *2a* 23–36, 22–25 apart. Inverted Y-shaped prosternal apodeme. 0 complete and 0–3 incomplete microtuberculate annuli between external genitalia and coxae. Genital coverflap 11–14, 18–21 wide, with 8–12 longitudinal ridges on one rank. Pregenital plate (sensu Flechtmann et al. 2015) present, with elongated tubercles in about four transverse rows arranged in more or less two transverse

areas with the basal two rows slightly rounded. Proximal setae of coxisternal plate III *3a* 7–13, 13–18 apart. Internal genitalia (Figure 7C) extending moderate distance forward.

Female

**Deutogynes:** not observed during this study.

Male

(*n* = 2)

Morphology similar to female, including presence or absence of setae. Only measurements are given here. Features are not described unless they differ from those of the female.

Idiosoma: 172–191 including pedipalp, 152–176 excluding gnathosoma, 50–55 wide (at the level of *c2* setae). Opisthosoma with 62–63 dorsal and 50–54 ventral microtuberculate annuli (from first annulus posterior to coxae II). Telosome dorsally with spiny microtubercles protruding from the posterior margin of the annuli. Opisthosomal setae *c2* 22–23 on ventral annulus 9, 48–51 apart; opisthosomal setae *d* 17–28 on ventral annulus 18–20, 37–40 apart; opisthosomal setae *e* 31–34 on ventral annulus 21–28, 24–25 apart; opisthosomal setae *f* 14–18, on annulus 4–5 from the rear, 16–17 apart, fine at apex. Opisthosomal setae *h1,* minute, less than 0.5. Opisthosomal setae *h2* 38-42, relatively long and finely tapered.

Gnathosoma: 21 long, chelicerae 17–19, pedipalp coxal setae *ep* 4–5, apico-ventral setae *v* 2–3.

**Prodorsal shield:** oval 23–24 long, 39–44 wide; scapular setae *sc* 18–21, 23 apart.

Leg I: 16–18, trochanter 3–4, femur 4, genu 3, antaxial genual setae *l″* 15; tibia 2–3; tarsus 4–5, paraxial unguinal tarsal seta *u′* 2, paraxial fastigial tarsal setae *ft′* 13, antaxial fastigial tarsal
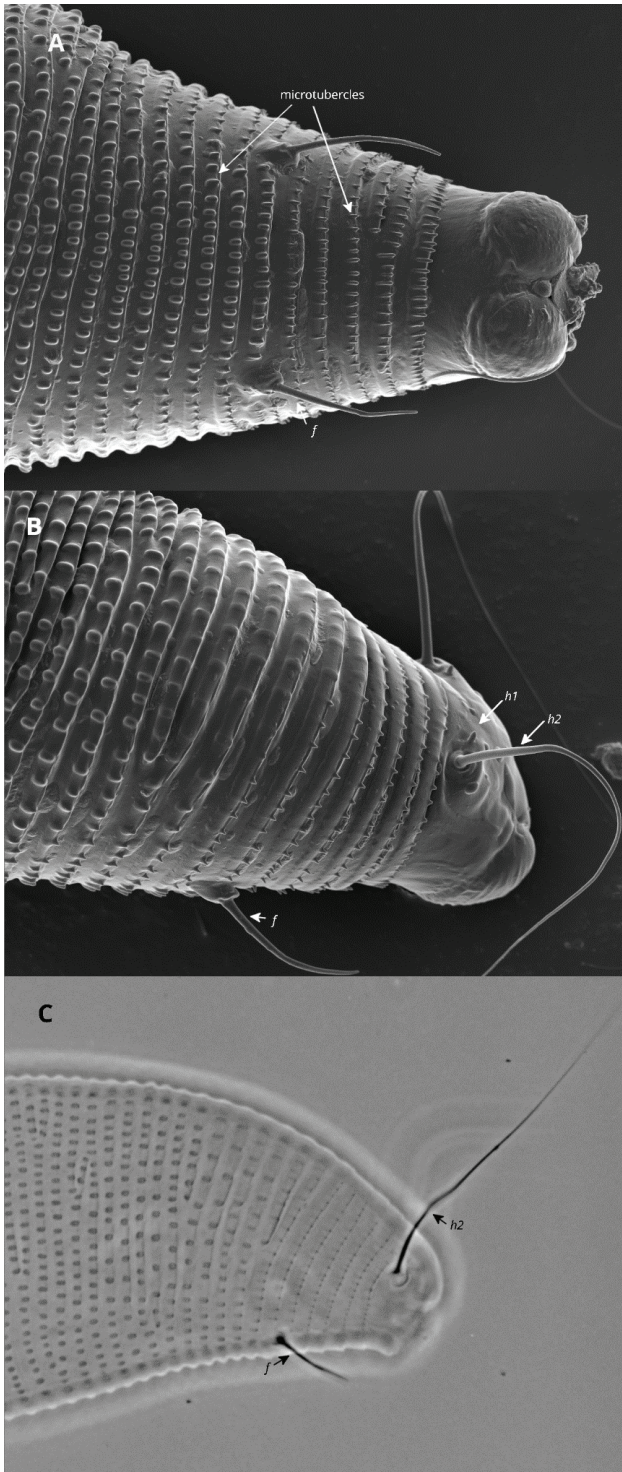
Figure 2. Caudal region, viewed by SEM in ventral (A) and lateral (B) view and by PCLM in lateral view (C). Microtubercles and setae are labelled, including the presence of the minute *h1* setae (B) which is very difficult to see using PCLM and was previously described as missing. SEM images were cropped to show the region of interest. PCLM images were taken with 100× oil objective. For sizes of structures, refer to the measurements included in the text.

setae *ft″* 7–8. Tarsal solenidion ω 6, tarsal empodium *em* 4–6, simple, symmetrical, 6-rayed.

Leg II: 17–18, trochanter 3, femur 4–5, basiventral femoral seta *bv* 3–4; genu 3, antaxial genual setae *l″* broken could not be measured; tibia 2.6, paraxial tibial setae *l′* absent; tarsus 4–5, paraxial unguinal tarsal seta *u′* 2, paraxial fastigial tarsal setae *ft′* 15–17, antaxial, fastigial tarsal setae *ft″* 3–4. Tarsal solenidion ω 7–7. Empodium *em* 4–5, simple, symmetrical, 6-rayed.
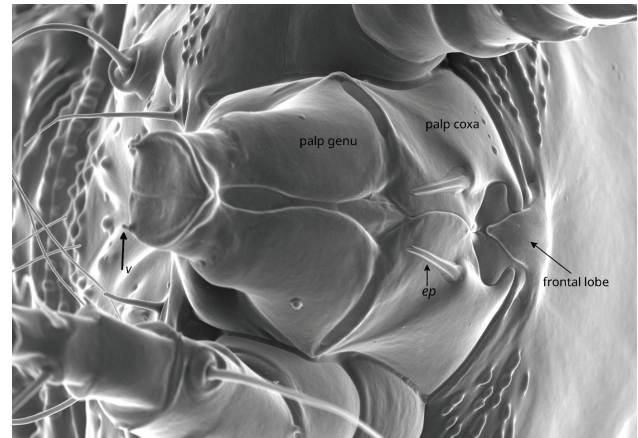
Figure 3. SEM image of the gnathosoma, showing the pedipalps with the segments labelled and the small frontal lobe originating from the prodorsal shield. Setae *v* and *ep* are labelled. The chelicerae are retracted within the pedipalps and cannot be seen in this image. SEM images were cropped to show the region of interest. PCLM images were taken with 100× oil objective. For sizes of structures, refer to the measurements included in the text.

Coxisternal area: (Figure 8) anterolateral setae on coxisternal plate I *1b* 4, 7 apart, proximal setae on coxisternal plate I *1a* 19–22, 11 apart, proximal setae on coxisternal plate II *2a* 16–19, 20–21 apart. 2 complete and 2 incomplete microtuberculate annuli between external genitalia and coxae. External genitalia 11 long, 15–16 wide, Proximal setae on coxisternal plate III *3a* 7 and 14–15 apart, with dense irregularly arranged granules posterior to 3a.

Nymph

(Figure 9) (*n* = 2)

Idiosoma: chunky and shorter than adults, translucent to whitish, wormlike body, 143–170 long including pedipalp, 47–52 wide (at the level of *c2* setae). Opisthosoma dorsally arched with 50–52 dorsal and 44–45 ventral semiannuli. Ventrally, few, scattered oval to round microtubercles arranged medially in a band about the width of the distance between setae *3a*, and approximately 10 μm on the inside of setae *d,* up to a short distance posterior to *d,* sometimes down to setae *f.* Dorsally, oval to round microtubercles spreading over a wider area compared to the ventral side, present medially in a band about the width of the distance between setae *sc* arranged in an hourglass shape. Opisthosomal setae *c2* 14–15, 43 apart on annulus 6–7, opisthosomal setae *d* 27–28, 32 apart on annulus 16; opisthosomal setae *e* 25–26, 19 apart on annulus 25; opisthosomal setae *f* 9–10, 15–16 apart on annulus 41, or on annulus 4–5 from the rear. Seta *h1* minute, seta *h2* 37–43.

Gnathosoma: 18–23, directed forward and slightly downward, chelicerae 17, pedipalp coxal seta *ep* 2–3, apico-ventral setae *v* 1–2, pedipalp genual setae *d* absent.

Prodorsal shield: 25–26 long, 39–43 wide, unlike adult, granules are not visible, faint admedian lines. Scapular setae *sc* 16–17, 22 apart, projecting posteriorly.

Leg I: All usual segments present, 14–15; trochanter 3, femur 4, basiventral femoral setae *bv* absent, genu 2–3, antaxial genual setae *l′* 13; tibia 2–3, paraxial tibial setae *l′* absent; tarsus 4.6, paraxial unguinal tarsal seta *u′* 1.4, paraxial fastigial tarsal setae *ft′* 3, antaxial fastigial tarsal setae *ft″* 10. Tarsal solenidion ω 4, slightly curved, blunt to slightly knobbed. Empodium *em* 3.5 simple, 5-rayed.

Leg II: All usual segments present, 13; trochanter 2, femur 3.5, basiventral femoral *bv* setae 2, genu 2, antaxial genual setae *l″* 10–16; tibia 2, paraxial tibial setae *l′* absent; tarsus 4, paraxial unguinal tarsal seta *u′* 1–2, paraxial fastigial tarsal setae *ft′* 3,
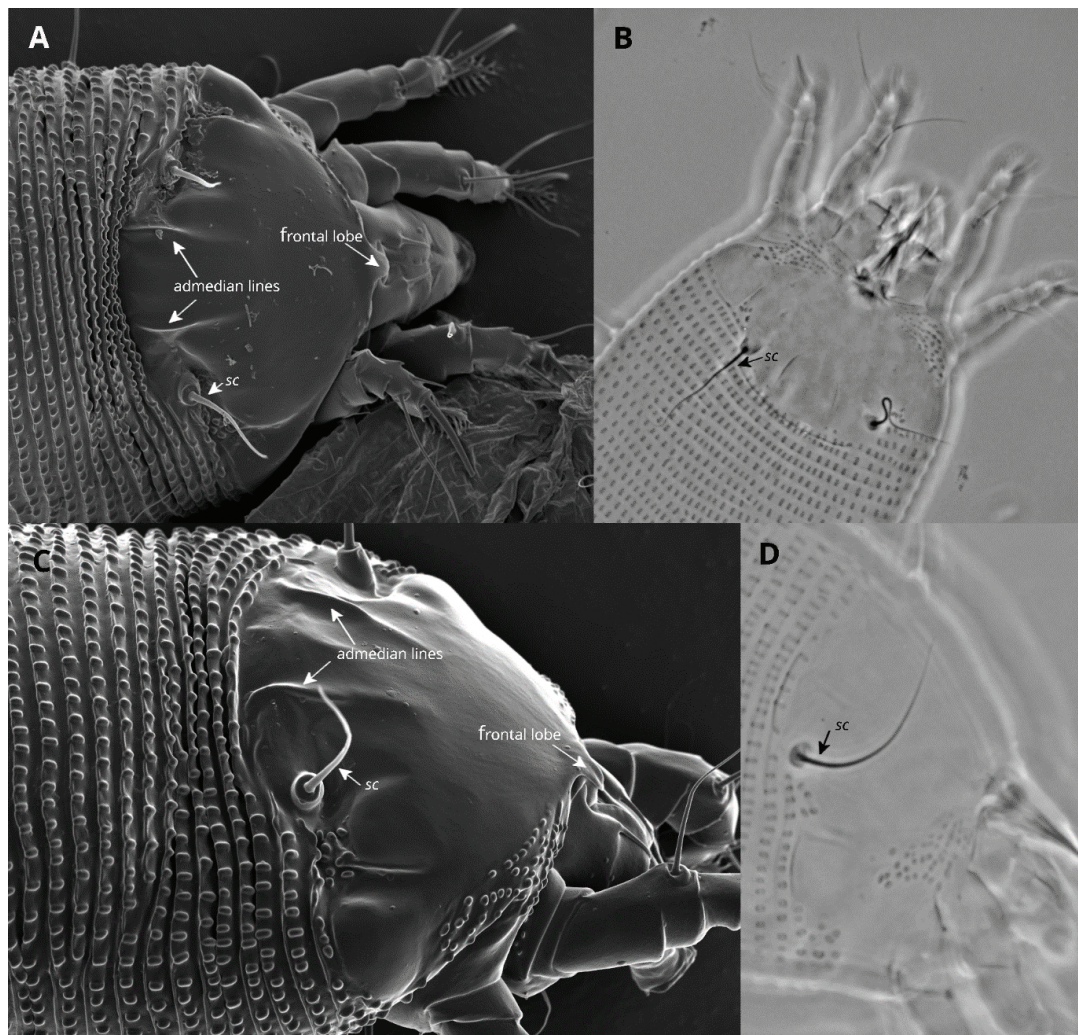
Figure 4. The prodorsal shield in dorsal (A and B) and lateral (C and D) view, as viewed by SEM (A and C) and PCLM (B and D). Setae *sc*, admedian lines and the frontal lobe are labelled. The eye-like area can be seen in lateral view with a band of granules on the outer margin. SEM images were cropped to show the region of interest. PCLM images were taken with 100× oil objective. For sizes of structures, refer to the measurements included in the text.
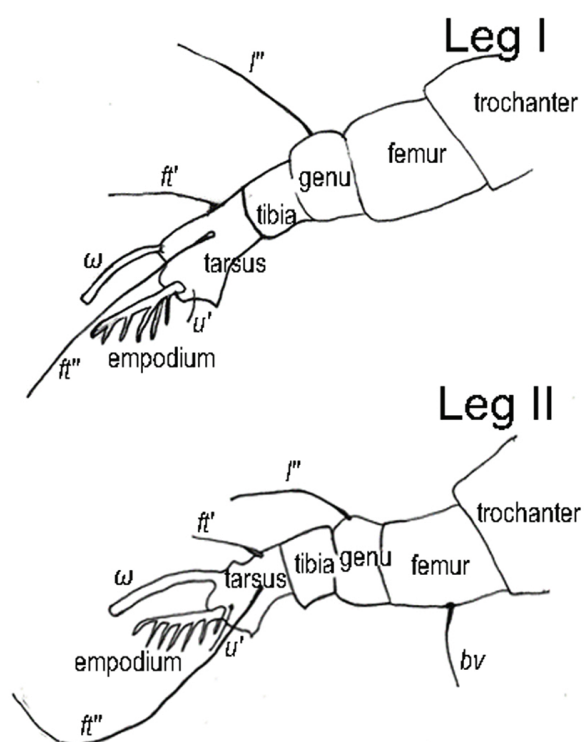
**Figure 5.** Schematic line drawings of Legs I and II showing the segments and setae names.

antaxial fastigial tarsal setae *ft″* 10. Tarsal solenidion ω 4–5, slightly curved, blunt to slightly knobbed. Empodium *em 3–4*, simple, 5-rayed.

Coxisternal area: suboral plate rounded, sometimes with faint curved lines, fewer granules than female adult. Prosternal apodeme not visible. Coxisternal plates I and II ornamented with very few granules. Anterolateral setae on coxisternal plate I *1b* 3, 7–8 apart, proximal setae on coxisternal plate I *1a* 11–12, 10 apart, proximal setae on coxisternal plate II *2a* 20–23, 19 apart. External genitalia absent. Proximal setae of coxisternal plate III *3a* 3–4, 8–9 apart.

### *Larva*

(Figure 10) (*n* = 2)

Idiosoma: transluscent, wormlike body 112–128 (including pedipalp), 52–55 wide. Opisthosoma dorsally arched with 29–31 dorsal and 30 ventral annuli. Opisthosomal microtubercles varied between specimens, and could be absent or present on dorsal, ventral or both surfaces. In dorsal view, when present, irregular shaped to pointed microtubercles scattered towards the rear end. In ventral view, when present, few oval to rounded microtubercles between *3a* and *e* setal-area. On both sides, the microtubercles were along setae *3a* and on the dorsal rear end. Opisthosomal setae *c2* 6, 50 apart on annulus 3 or 4, opisthosomal setae *d* 6, 28 apart, on annulus 10–11; setae *e* 3 long, 19 apart on annulus 16; setae *f* 8 long, 15–16 apart on annulus 26–27, or annulus 4 from the rear. Setae *h2* 23 long, Setae *h1* minute.
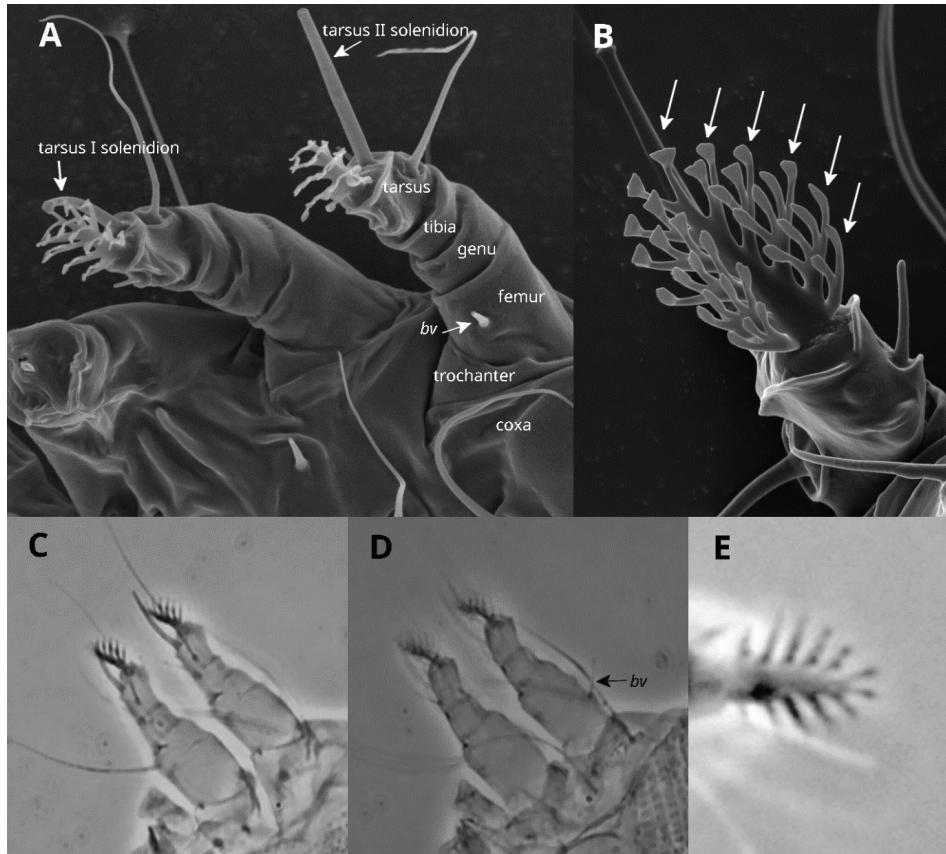
Figure 6. Legs I and II (A, C and D) and empodia (B and E) viewed by SEM (A and B) and PCLM (C, D and E). Leg segments are labelled (A), as well as femoral II setae **bv** which was previously described as missing. The six empodial rays are indicated by arrows (B). In PCLM images, features may only be visible at different focal points (C and D). SEM images were cropped to show the region of interest. PCLM images were taken with 100× oil objective. For sizes of structures, refer to the measurements included in the text.
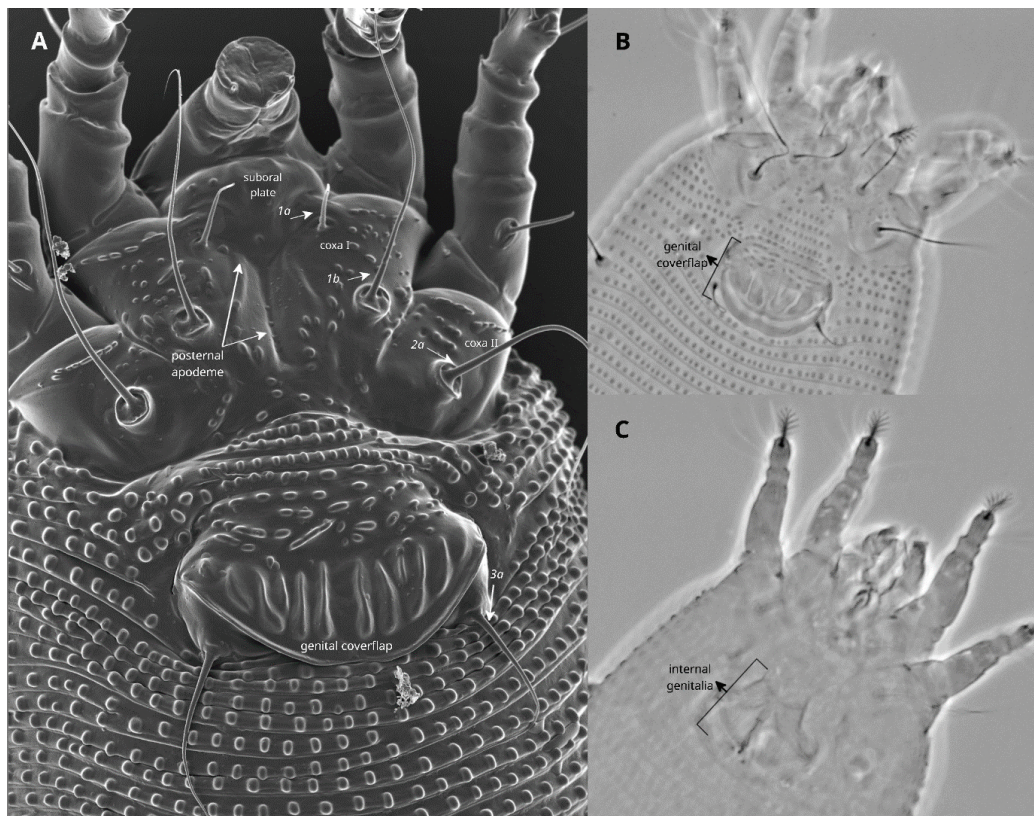
Figure 7. The coxisternal area of the protogyne female, viewed by SEM (A) and PCLM (B and C). External features, including the genital coverflap with ridges in a single rank (row) and setae are labelled (A and B). C shows the shape of the internal genitalia, only visible with PCLM. SEM images were cropped to show the region of interest. PCLM images were taken with 100× oil objective. For sizes of structures, refer to the measurements included in the text.
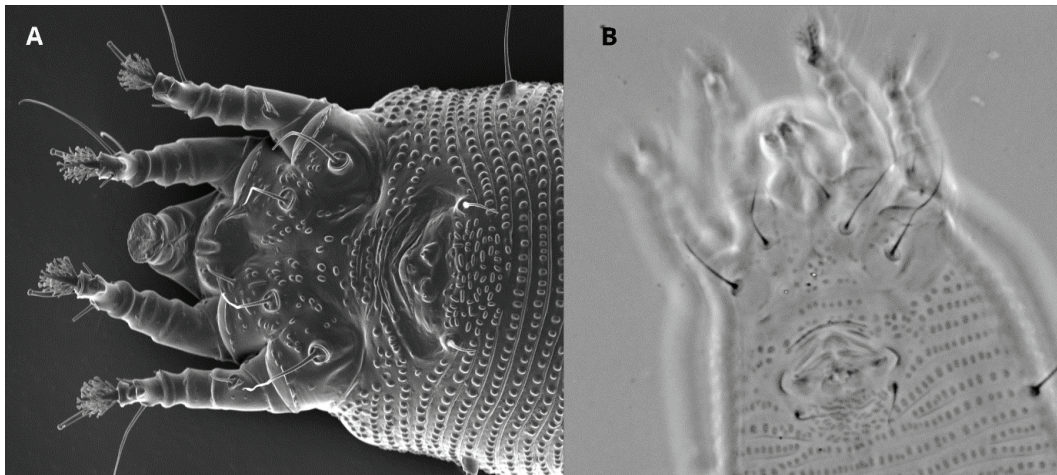
Figure 8. The coxisternal area of the male, viewed by SEM (A) and PCLM (B). External features and setal arrangement are as for the female (Figure 6), except for the genitalia and genital coverflap, which is not present in the male. SEM images were cropped to show the region of interest. PCLM images were taken with 100× oil objective.
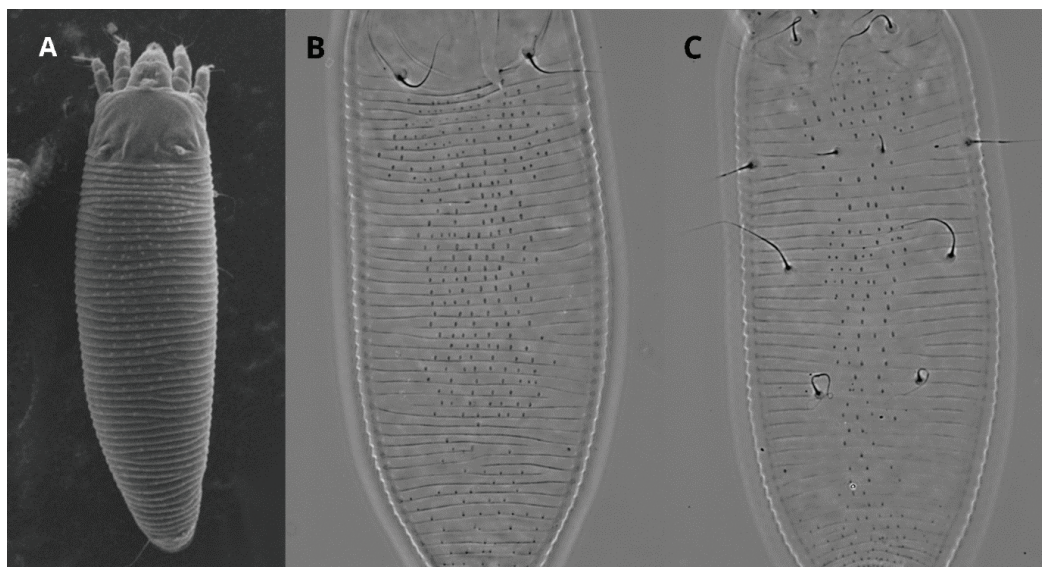
Figure 9. Nymph, viewed by SEM (A) and PCLM in dorsal (B) and ventral (C) view. Setal arrangement is as for the adult. Dorsally, microtubercles form an hourglass shape approximately the width of **sc – sc** (A and B)**.** Ventrally, microtubercles are arranged in a band about the width of **3a – 3a** (C)**.** SEM images were cropped to show the region of interest. PCLM images were taken with 100× oil objective. For sizes of structures, refer to the measurements included in the text.
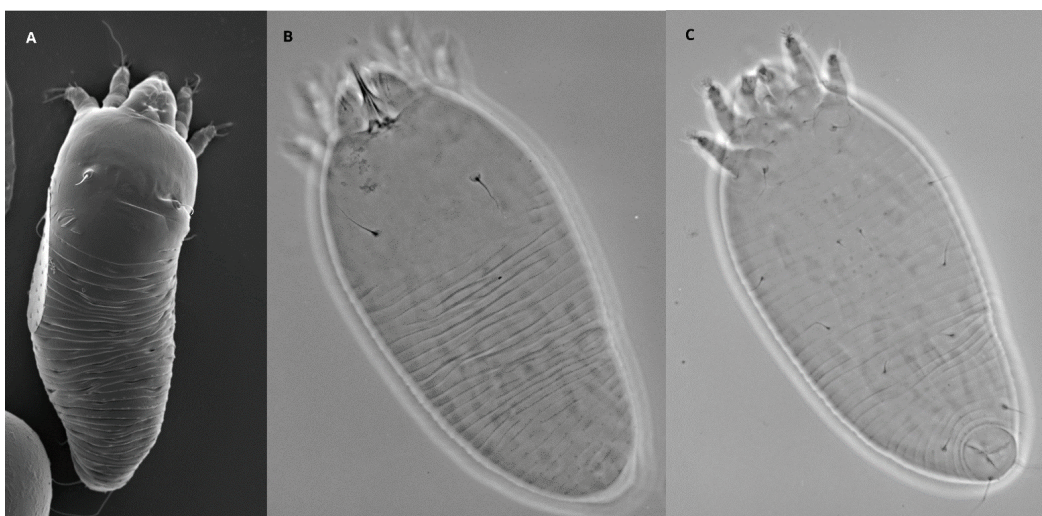

Figure 10. Larva, viewed by SEM (A) and PCLM (B and C), showing dorsal (A and B) and ventral (C) aspects. SEM images were cropped to show the region of interest. PCLM images were taken with 100× oil objective. For sizes of structures, refer to the measurements included in the text.

Gnathosoma: 14–15, slightly bent. Chelicerae 11–13, pedipalp coxal setae *ep* 3, apico-ventral setae *v,* not visible for measurements. Pedipalp genual setae *d* absent.

Prodorsal shield: prodorsal shield smooth, 19–21 long, 32–37 wide, admedian lines and granules not visible. Scapular setae *sc* 8–9, 20 apart, projecting posteriorly.

Leg I: all usual segments, 12–13; trochanter 3–4, femur 3–4, genu 3, antaxial genual setae *l″* 13; tibia 2–3, tibial setae *l′* absent; tarsus 3, paraxial unguinal setae *u′* 2, paraxial fastigial tarsal setae *ft′* 5–6, antaxial fastigial tarsal setae *f″* 9–10. Tarsal solenidion ω 4, slightly curved, blunt to slightly knobbed. Empodium *em* 3–4, simple, 3-rayed.

Leg II: all usual segments, 11; trochanter 2-3, femur 3, basiventral femoral seta *bv* 3, genu 2, antaxial genual setae *l″* 14; tibia 1, tarsus 3, paraxial unguinal tarsal seta *u′* 1, paraxial fastigial tarsal setae *ft′* 4, antaxial fastigial tarsal setae *ft″* 9–11. Tarsal solenidion ω 5–6, slightly curved, blunt to slightly knobbed. Empodium *em* 3, simple, 4-rayed.

Coxisternal area: suboral plate rounded, sometimes with faint curved lines, fewer granules than female adult. prosternal apodeme not visible. Coxisternal plates I and II ornamented with very few granules. Anterolateral setae on coxisternal plate I *1b* 2, 6–7 apart, proximal setae on coxisternal plate I *1a* 4, 8–9 apart, proximal setae on coxisternal plate II *2a* 8–9, 16–19 apart. External genitalia absent. Proximal setae of coxisternal plate III *3a* 2, 6 apart.

Material examined

Specimens observed for qualitative features: 38 females, 16 males, 28 nymphs, 13 larvae, Dullstroom farm, MP, SA March 2015 – May 2016; 24 females, 10 males, 18 nymphs, 8 larvae, Lydenberg farm, MP, SA March 2015 – May 2016; 425 females, 74 males, 163 nymphs, 60 larvae, Amsterdam farm, MP, SA November 2014 – May 2016. See Table 2 for further details.

Specimens for measurements

All specimens were collected from Amsterdam farm in Mpumalanga, South Africa.

- 6 females (slides 47803 & 47806) collected in March 2015,
- 5 females (slides T1S12, T2S19, T2S20) collected in July 2015,
- 2 males (slides T1S3; T1S11) collected in August 2015,
- 2 nymphs (slides T1S5, T1S6) collected in March 2015, and
- 2 larvae (slides T2S14, T2S16) collected in November 2014.

Principal component analysis (PCA)

The PCA revealed no clear clustering of individuals, nor a strong influence from any single component or character (Figure S1 in Supplementary Material). PCA1 and PCA2 explained 51.5% of the total variation (32.94% and 18.53%, respectively) (Table S2 in Supplementary Material). PCA1 was strongly influenced by characters associated with length: idiosomal length, position of ventral setae *e*, *d* and *f*, and gnathosomal length were the main components. PCA2 was influenced more by setal lengths, with leg I seta *f′*, coxal seta *2a* and ventral seta *e* lengths being the most influential (Table S2 in Supplementary Material).

Remarks

Female measurements included individuals collected in winter and summer seasons. On average, females collected in winter appeared to be a bit longer and larger than females collected in summer. There was no clear distinction in measurements of individual characters between individuals of different seasons (Table S1 in Supplementary Material).

Identification key to Eriophyoidea known on *Vaccinium* species worldwide

This key is based on morphological features visible on slide-mounted specimens viewed under PCLM. Note that this is not a dichotomous key, and some points have more than two options.

1. Gnathosoma large in comparison to body. Cheliceral stylets relatively long, abruptly bent down near base. Empodia often large, entire or divided. Female genital coverflap usually smooth, female genital apodeme of moderate length, often narrowed anteriorly ....Diptilomipidae Keifer 1944 (1 species)

    Prodorsal shield wide with ridges, complete median and admedian lines, submedian lines incomplete, four cells on each side of anterior shield, horned projection present near median shield rear margin. Empodium 5-rayed and divided. Tarsal solenidion knobbed, *bv* absent. Genital coverflap with basal granules and 14 distal ridges. Short dorsal median ridge, smooth dorsal annuli, ventral annuli with rounded microtubercles. Sternal line, coxal area sculpted with granules, prosternal apodeme present. Vagrant on the underside of leaves of *Vaccinium bracteatum* ....
    ....*Diptacus bracteatus* Li, Wei and Qin 2009
   - Gnathosoma usually small in comparison to body, with short straight or slightly curved chelicerae, pedipalps with terminal segments short and truncate, enclosing the short-form oral stylet. Empodia usually simple. Genital coverflap usually with ridges. Eriophyidae Nalepa 1898 (8 species on *Vaccinium*) 2

2. Vermiform mites, annuli subequal dorsoventrally. Frontal lobe typically absent, or with a light projection over gnathosoma base. If frontal lobe present, then it is narrow, basally flexible, and combined with narrow annuli. Genital apodeme usually of moderate anterior length ....
    ....Eriophyinae Nalepa 1898a (1 species) (Nalepa 1898).

    No opisthosomal ridges. Leg I with basiventral femoral seta and paraxial tibial setae absent. Forecoxae often confluent. Coxal setae *2a*, *1a* and *1b* present. Genital coverflap with 8–10 ridges in a single rank. Empodium 6-rayed. Tarsal solenidion slightly knobbed. Prodorsal shield without strong central lines. Inverted Y-shaped prosternal apodeme, rounded, granulate suboral plate. In buds of *Gaylussacia baccata* and *Vaccinium* species ....*Acalitus vaccinii* (Keifer 1939)
   - Fusiform mites, annuli typically dorsoventrally differentiated (broad dorsal annuli and narrow ventral annuli). Frontal lobe typically present, broad-based and rigid. Female genital apodeme usually extending moderate distance forward. Female genitalia usually not appressed to coxae and, in lateral view, lying on level with venter. Genital coverflap variably ornamented, ridges typically occur in one (rarely 2) ranks. Phyllocoptinae Nalepa 1892b (7 species) 3

3. Scapular setal tubercles usually set ahead of prodorsal shield rear margin, directing setae *sc* anteriorly, dorsally or convergently. Opisthosoma with a single middorsal ridge or with 3 or more longitudinal ridges with prominent middorsal ridge. Middorsal ridge ending in a broad furrow before termination of suboral ridges. Opisthosomal dorsum flattened in cross section. Prodorsal shield without frontal lobe. *Calepitrimerus* Keifer, 1938 (3 species) 4
   - Scapular setal tubercles set ahead or near prodorsal shield rear margin, directing setae *sc* forward or up, medially or convergently posteriad. Opisthosoma evenly arched, round in cross section, and less sharply tapered posteriorly. Opisthosomal shape variable: broad dorsal

semi-annuli and narrow ventral semi-annuli, or with little dorsoventral differentation. Prodorsal shield with frontal lobe. *Phyllocoptes* Nalepa 1887 (4 species) 5

4. Wax stripes along the ridges. Prodorsal shield with a central ridge extending back and ending just beyond the dorsal tubercles setting. Broad and blunt frontal lobe, setae *sc* projecting up and ahead, setae *h1* absent. Empodium 3-rayed. Smooth annuli. Genital coverflap with 8–9 ridges and weak horizontal markings at the top. Around the lateral buds of fresh succulent twigs of *Vaccinium ovatum* ....*Calepitrimerus gilsoni* Keifer 1953

    –   Prodorsal shield pattern obscure or virtually absent. Frontal lobe with spines. *sc* setae projecting up and forward. Genital coverflap with 6–8 ridges, prosternal apodeme moderately long. Setae *h1* present. Empodium 6-rayed. Vagrants on both sides of leaves of *Vaccinium atrococcum* ....*Calepitrimerus darrowi* Keifer, 1940

    –   Prosordal shield with lateral lines and granules, median line absent, admedian lines curving back, submedian lines curving back from side of anterior shield lobe and joining with *sc* tubercles. Annuli with fine and elongate microtubercles. Weak middorsal opisthosomal ridge extends back to 25th–30th dorsal annuli. Coxae ornamented with curved lines and granules, prosternal apodeme divided and short. Genital cover flap with two ranks of faint parallel markings at the top and 8 weak longitudinal ridges at the bottom. Vagrants on both sides of leaves of *Vaccinium parvifolium* ....*Calepitrimerus olympici* Keifer,1971

5. Flattened wedge-shaped body. Empodium on leg I 4-rayed, leg II 6-rayed. Genital coverflap with 6 ridges. Vagrant on upper leaf surface of *Vaccinium amoenum* ....*Phyllocoptes vandinei* Keifer, 1940

    –   Empodium 4- or 5-rayed, same number on leg I and II. Genital coverflap with 8–10 ridges 6

6. Flattened body. Empodium 5-rayed. Genital coverflap with 8 ridges. Unforked sternal line. *h1* setae 5µm. Legs with knobbed solenidion. Vagrant on the underside of leaves of *Vaccinium oxycocci* ......*Phyllocoptes oxycocci* Roivainen, 1947

    –   Empodium 4-rayed. Genital coverflap with 10 ridges. *h1* setae minute 7

7. Fusiform body shape, broad and short, 65–70 µm wide, 170–180 µm long. Prosternal apodeme indistinctly forked. Genital coverflap with 10 ridges. Legs with curved and knobbed solenidion. Vagrant on the underside of leaves of *Vaccinium vitisidaea* ....*Phyllocoptes vitisidaeae* Roivainen 1951

    –   Body shape narrow and long, 42–46 µm wide, 185-220 µm long. Genital coverflap with 10 ridges. Empodium 4-rayed. Vagrant on leaves of *Myrtillus uliginosa, M. nigra* and *Vaccinium myrtillus* ....*Phyllocoptes vaccinii* (Flögel & Goosmann, 1933)

Genetic analyses

A number of DNA extractions failed to yield PCR amplicons, or once sequenced were of such poor quality as to be unusable. Ultimately, three eriophyoid samples from Dullstroom farm (D2, D3 and D4) yielded good quality DNA sequences for both regions. These were deposited in GenBank with accession numbers MW246114, MW246115 and MW246116 for the D2-28S fragment and MW250771, MW250772 and MW250773 for the COI fragment. These sequences showed no intraspecific variation.

A blastn search for the 28S sequences MW246114-6 (all identical) returned sequence OQ737114.1 of *Nothopoda* sp. (Eriophyidae), (28S, 100% coverage, 78.24% identity) as the best hit when sorted by E-value, and *Quadracus urticarius* (Diptilomiopidae), KY921996.1 (28S, 48% coverage, 94.83% identity) as the best hit when sorted by percent identity.

A blastn search for the COI sequences MW250771-3 (all identical) returned sequence MN905284.1 of *Trisetacus* sp. (Phytoptidae), (COI, 63% coverage, 81.11% identity) as best hit, followed by *Aculus* sp. (Eriophyidae), MW439280.1, (COI, 70% coverage, 79.46% identity) when sorted by either E-value or percent identity.

Blastx of the COI sequences returned sequence WLI54571.1 of *Leipothrix* sp. (Eriophyidae) as the best hit (COI, 100% coverage, 76.98% identity) when sorted by either E-value or percent identity. Only two other *Acalitus* species (*A. phloeocoptes* and *A. rudis*) have sequences available on GenBank, neither of which have sequences for regions that overlap with those sequenced in the current study.

DISCUSSION

Acalitus vaccinii occurs on wild and cultivated blueberry, causing significant economic damage on susceptible varieties in its native distribution. The damage seen due to *A. vaccinii* on South African blueberry was significant, with yield losses ranging from 30–90% (Craemer 2018). When *A. vaccinii* was first identified in South Africa it was noted that the description of this mite needed revision (Craemer 2018). Available descriptions did not include all life stages, and important morphological features had not been noted or were inadequately described. No comprehensive key to *Acalitus* species nor eriophyoid species on blueberry was available. Here we rectified these omissions by providing accurate details of key features of multiple life stages.

In the original description of *A. vaccinii* by Keifer (1939), some key morphological features were omitted in both the drawing and text description. Most importantly these included the *h1* (accessory) setae, leg I & II *u'* (mesal) setae and leg II *bv* (femoral setae) that are considered taxonomically important as the presence or absence of setae may be an indication of a different species (Amrine and Manson 1996; De Lillo 2010). Keifer measured 33 female and 5 male (without description and drawing) characteristics, as compared to the 75 characters measured for females, 69 for males and 68 for immatures in this study.

Many of the features not included in the original description are minute and may have been missed in original observations. For example, the observation of the setae mentioned above in the current study may largely be due to advancements in microscopy since the original description. The Scanning Electron Microscopy (SEM) technique, specifically Low-temperature SEM (LT-SEM), used here was able to substantially increase visual detail of *A. vaccinii* including these minute structures. LT-SEM also eliminated uncertainties in the shape of structures, especially when viewing the *h1* setae, empodium and other subtle features such as the frontal lobe and shape of microtubercles.

In addition to Keifer (1939), Baker and Neunzing (1970) described the immatures of *A. vaccinii*. Differences observed between the former and this study is in the presence and arrangement of the opisthosomal microtubercles in immatures. The original description presented the larva without micro-tubercles and the nymph with microtubercles covering the entire opisthosoma. In the present study, on nymphs, the ventral microtubercles were arranged medially about the width of *3a – 3a* setae and the dorsal microtubercles were arranged in an hourglass shape medially about the width of *sc – sc* setae and were more widely spaced than those on the ventral side. On larvae, microtubercles were variously present or absent on either the dorsal, ventral or both surfaces, with variable non-uniform arrangements. These observations may be a result of intraspecific variations due to a limited number of studied specimens in previous studies and advances in microscopy encouraging qualitative and quantitative analysis. Many measurements that are standard for modern descriptions were not presented by Baker and Neunzing (1970) for the immature

life stages. Additionally, the 35 measurements presented in that study cannot be used for comparison with current standards and procedures, as measurement techniques were not stipulated.

The presence of all life stages (females, males, immatures and eggs) of *A. vaccinii* on cultivated blueberries confirmed that the crop is an obligate host. Specimens were collected and studied throughout the year to capture variation and in attempt to detect the presence of a deutogyne, should one exist. A deutogyne is a winter form of eriophyoid mite and was detected in North America for *A. vaccinii* (Baker et al. 1996; Manson and Oldfield 1996; Cromroy and Kuitert 2001). It is important to establish whether both forms of a species occur in a particular area to avoid future misidentification of the deutogyne as a separate species (or even genus) because of morphological differences (Zhao 2000; Smith et al. 2010; Guo et al. 2015). Although females collected in winter appeared, on average, larger than the summer specimens, this was not uniform and did not form a separate cluster when analysed by PCA (Figure S1 in Supplementary Material). Other characters did not differ between winter and summer specimens. Further, immature life stages and males were collected in all seasons. Thus, morphological differences and biological evidence do not prove without doubt the presence of a deutogyne in South Africa. The absence of deutogynes in SA might be explained by the mild winter conditions of Mpumalanga (8–19 °C) (South African Weather Service, 2018), in comparison to the mite's native range (–1 to –7 °C) (www.usclimatedata.com/climate/united–states/us). The lack of deutogynes and the viability of all life stages through the winter season might have contributed to the increased population size and significant crop injury at the Mpumalanga farm. This also suggests that the mite is likely to be a more serious pest in warmer regions of blueberry production. In addition to the enhanced morphological descriptions added here, sequence information for two DNA regions commonly used in mite species identifications were made available on GenBank to aid future identification. Partial sequences of the COI gene are routinely used for identification of many animal species including mites, and the D2 region of 28S rDNA has shown differences between eriophyid species within a genus (Skoracka and Dabert 2010). In conjunction, these regions have potential for identification of *A. vaccinii* and other eriophyoid species. It will be of great benefit if more sequences were generated and deposited in GenBank to increase the pool of sequences for molecular identification of eriophyoid mites.

This study supplemented and enhanced the previous descriptions of *A. vaccinii* to enable more accurate identification and ease of comparison when conducting taxonomic analyses on this important group. Importantly, additional characters (including two DNA barcodes), morphological measurements and some life stages that were not included in previous descriptions are here presented in detail. The use of complementary morphological and molecular techniques greatly enhanced our ability to see and image minute characters and provide additional information and it is recommended that future workers on this group do the same.

ACKNOWLEDGEMENTS

AUTHOR CONTRIBUTIONS

NP Ngubane-Ndhlovu: Investigation; Writing – original draft
I Dhanani: Genetic analyses investigation
F Roets: Supervision; Writing – review and editing
DL Saccaggi: Supervision; Writing – review and editing

ORCID IDS

NP Ngubane-Ndhlovu: https://orcid.org/0000-0001-8947-7486
F Roets: https://orcid.org/0000-0003-3849-9057
DL Saccaggi: https://orcid.org/0000-0002-5706-2697

SUPPLEMENTARY MATERIAL

There is supplementary material available with this article.

REFERENCES

Amrine Jr JW, Manson DCM. 1996. Preparation, mounting and descriptive study of eriophyoid mites. In: Lindquist E, Sabelis MW, Bruin J, editors. Eriophyoid Mites: Their Biology, Natural Enemies and Control. Amsterdam: Elsevier Science Publishers; pp 383–396.

Amrine Jr JW, Stasny TAH, Flechtmann CHW. 2003. Revised keys to world genera of Eriophyoidea (Acari: Prostigmata). Michigan: Indira Publishing House; 244 pp.

Baker EW, Kono T, Amrine, JW Jr, Delfinado-Baker, MD, Stasny T. 1996. Eriophyoid mites of the United States. USA: Indira Publishinga House; 349 pp.

Baker JR, Neunzing HH. 1970. Biology of the blueberry budmite. Journal of Economic Entomology 63: 74–79.

Chetverikov PE, Craemer C. 2015. Gnathosomal interlocking apparatus and remarks on functional morphology of frontal lobes of eriophyoid mites (Acariformes, Eriophyoidea). Experimental and Applied Acarology 66: 187–202. https://doi.org/10.1007/s10493-015-9906-3

Chetverikov PE, Desnitskaya EA, Efimov PG, Bolton SJ, Cvrković T, Petanović RU, Zukoff S, Amrine JW, Klimov P. 2019. The description and molecular phylogenetic position of a new conifer-associated mite, *Setoptus tsugivagus* n. sp. (Eriophyoidea, Phytoptidae, Nalepellinae). Systematic and Applied Acarology 24: 683–700. https://doi.org/10.11158/saa.24.4.13 10.11158/saa.24.4.13

Craemer C. 2018. First record, current status, symptoms, infested cultivars and potential impact of the blueberry bud mite, *Acalitus vaccinii* (Keifer) (Prostigmata: Eriophyidae) in South Africa. Acarologia 58: 735–745.

Cromroy, HL, Kuitert LC. 2001. Common name: Blueberry bud mite, scientific name; *Acalitus vaccinii* (Keifer) (Arachnida: Acari: Eriophidae). DPI Entomology Circular: 130.

Dabert M, Witalinski W, Kazmierski A, Olszanowski Z, Dabert J. 2010. Molecular phylogeny of acariform mites (Acari, Arachnida): Strong conflict between phylogenetic signal and long-branch attraction artifacts. Molecular Phylogenetics and Evolution 56: 222–241. https://doi.org/10.1016/j.ympev.2009.12.020

De Lillo E, Craemer C, Amrine JW, Nuzzaci G. 2010. Recommended procedures and techniques for morphological studies of Eriophyoidea (Acari: Prostigmata), In Eriophyoid Mites: Progress and Prognoses.

Echlin P, Paden R, Dronzek B, Wayte R. 1970. Scanning electron microscopy of labile biological material maintained under controlled conditions., *In* Procedings of the 3rd. Annual Scanning Electron Microscopy Symposium; pp 49–56.

Flechtmann CHW, Arana M, Ciarrocchi F, Chetverikov PE, Amrine Jr. JW. 2015. Rediscovery and redescription of two eriophyid mites (Acari, Prostigmata, Eriophyidae) from *Baccharis salicifolia* (Asteraceae), from Argentina with remarks on the eriophyoid coverflap base. Acarologia 55: 387–396.

Folmer O, Black M, Hoeh W, Lutz R, Vrijenhoek R. 1994. DNA primers for amplification of mitochondrial cytochrome c oxidase subunit I from diverse metazoan invertebrates. Molecular marine biology and biotechnology 3: 294–299.

Guo J, Sadeghi H, Gol A, Xue X. 2015. A new species of the genus *Vittacus* Keifer (Acari: Eriophyidae) from Iran. Persian Journal of Acarology 4: 57–63. https://doi.org/10.22073/pja.v4i1.10187

Hedin MC, Maddison WP. 2001. A combined molecular approach to phylogeny of the jumping spider subfamily Dendryphantinae (Araneae: Salticidae). Molecular Phylogenetics and Evolution 18: 386–403. https://doi.org/10.1006/mpev.2000.0883

Horikoshi M, Tang Y 2018. ggfortify: Data Visualization Tools for Statistical Analysis Results. https://CRAN.R-project.org/package=ggfortify

Keifer H. 1938. Eriophyid studies II. Bulletin of Carlifornia Department of Agriculture 27: 301–323.

Keifer H. 1939. Eriophyid studies V. Bulletin of Carlifornia Department of Agriculture 28: 328–345.

Keifer H. 1940. Eriophyid studies. Bulletin of Carlifornia Department of Agriculture 29: 160–179.

Keifer H. 1944. Eriophyid studies XIV. Bulletin of Carlifornia Department of Agriculture 33: 18–38.

Keifer H. 1946. A Review of North American Economic Eriophyid Mites. Journal of Economic Entomology 39: 563–570. https://doi.org/10.1093/jee/39.5.563

Keifer H. 1953. Eriophyid Studies XXI. Bulletin of Carlifornia Department of Agriculture 42: 65–79.

Keifer H. 1965. Eriophyid studies B-13. Bulletin of Carlifornia Department of Agriculture 54: 1–20.

Keifer H. 1971. Eriophyid studies. Bulletin of Carlifornia Department of Agriculture 60: 1–24.

Keifer H. 1975. Injurious eriophyoid mites. In: Jeppson LR, Keifer HH, Baker EW, editors. Mites injurious to economic plants. Berkeley, California: University of California Press; pp 327–533.

Lindquist E, Amrine AJW. 1996. Systematic diagnosis for major taxa, and keys to families and genera with species on plant of economic importance. In: Lindquist EE, Sabelis MW, Bruin J, editors. World Crop Pests: Eriophyoid mites-Their Biology, Natural enemies and control. Amsterdam: Elsevier Science Publishers; pp 33–87.

Lindquist EE. 1996. External anatomy and notation of structures. In: Lindquist EE, Sabelis MW, Bruin J, editors. World Crop Pests: Eriophyoid mites-Their Biology, Natural enemies and control. Amsterdam: Elsevier Science Publishers; pp 3–31.

Manson DCM, Oldfield GN. 1996. Life forms, deuterogyny, diapause and sesonal development. In: Lindquist EE, Sabelis MW, Bruin J, editors. World Crop Pests: Eriophyoid mites-Their Biology, Natural enemies and control. Amsterdam: Elsevier Science Publishers; pp 173–183.

Meyer HJ, Prinsloo N. 2003. Assessment of the Potential of Blueberry Production in South Africa. Small Fruits Review 2: 3–22.

Nalepa A. 1887. Die Anatomie der Phytopten. Sitzungsberichte der Kaiserlichen Akademie der Wissenschaften 96: 115–165.

Nalepa A. 1892. Neue Arten der Gattung Phytoptus-Duj und Cecidophyes. Denkschriften der Kaiserlichen Akademie der Wissenschaften 59: 525–540.

Nalepa A. 1898. Zur Kenntniss der Gattung Trimerus Nalepa. Zoologische jahrbucher 11: 405–411.

Ngubane-Ndhlovu NP, Collet IJ, Saccaggi D. 2018. New quarantine mites detections in South Africa. In: XV International Congress of Acarology. Antalya. pp. 247

Roivainen H. 1947. Eriophyid news from Finland. Acta Entomologica Fennica 3: 1–51.

Roivanen H. 1951. Contributions of the knowledge of eriophyidae of Finland. Acta Entomology 8: 1–72.

RStudio Team. 2020. RStudio: Integrated Development for R. RStudio, PBC, Boston, MA. http://www.rstudio.com/.22 Jan 2024

Simon C, Frati F, Beckenbach A, Crespi B, Liu H, Flook P. 1994. Evolution, weighting, and phylogenetic utility of mitochondrial gene sequences and a compilation of conserved polymerase chain reaction primers. Annals of the Entomological Society of America 87: 651–701. https://doi.org/10.1093/aesa/87.6.651

Skoracka A, Dabert M. 2010. The cereal rust mite Abacarus hystrix (Acari: Eriophyoidea) is a complex of species: Evidence from mitochondrial and nuclear DNA sequences. Bulletin of Entomological Research 100: 263–272. https://doi.org/10.1017/S0007485309990216

Smith L, de Lillo E, Amrine JW. 2010. Effectiveness of eriophyid mites for biological control of weedy plants and challenges for future research. Experimental and Applied Acarology 51: 115–149. https://doi.org/10.1007/s10493-009-9299-2

Sonnenberg R, Nolte A, Tautz D. 2007. An evaluation of LSU rDNA D1-D2 sequences for their use in species identification. Frontiers in Zoology 4: 1–12. https://doi.org/10.1186/1742-9994-4-6

Tang Y, Horikoshi M, Li W 2016. ggfortify: Unified Interface to Visualize Statistical Result of Popular R Packages. The R Journal 8(2): 474–485. https://doi.org/10.32614/RJ-2016-060

Wickham H. 2016. ggplot2: Elegant Graphics for Data Analysis. Springer-Verlag New York. https://ggplot2.tidyverse.org

Wei S, Wang G, Li D, Qin A. 2009. Four new species of the genus Diptacus Keifer, 1951 from Guangxi, South China (Acari: Diptilomiopidae). International Journal of Acarology 35: 149–159. https://doi.org/10.1080/01647950902980096

Zhao S. 2000. Study of dispersal and diversity of eriophyoid mites (Acari: Eriophyoidea). PhD Thesis, West Virginia University, United States.